Early Stages of Film Creation in Thin Diblock Copolymer Films

P. Müller-Buschbaum,*,† J. S. Gutmann,‡ C. Lorenz-Haas,§ B. Mahltig,‡ M. Stamm,‡ and W. Petry†

Physik-Department, LS E13, TU München, James-Franck-Str.1, 85747 Garching, Germany; Institut f. Polymerforschung Dresden e.V., Hohe Str. 6, 01069 Dresden, Germany; and Max-Planck-Institut für Polymerforschung, Ackermannweg 10, 55128 Mainz, Germany

Received December 21, 2000; Revised Manuscript Received July 17, 2001

ABSTRACT: Thin poly(styrene-*block*-*p*-methylstyrene) diblock copolymer films on top of silicon substrates were examined right after preparation and during the early stages of annealing. Using specular and off-specular X-ray scattering as well as scanning force microscopy, the film morphology is determined. With the spin-coating technique films are prepared which exhibit a roughness correlation between the substrate and the copolymer surface within a limited film thickness and molecular weight range right after preparation. The transferred part of the roughness spectrum of the substrate is probed and explained as a morphology of a frozen liquid with a surface bending rigidity. During annealing the energetically unfavorable roughness replication decays, and an internal ordering is formed. The decay of long-range correlation is explained by a surface diffusion where diffusion is slowed down as compared to bulk behavior.

Introduction

Diblock copolymers are macromolecules consisting of two coupled chemically different polymer species A and B. In the bulk due to block segregation and microphase separation diverse ordered morphologies such as lamellae, cylinders, spheres, and bicontinuous minimal-surface microstructures occur. These ordered morphologies exhibit properties that differ considerably from those of the disordered state.[1] Various morphologies have been investigated as a function of block ratio, molecular weight, temperature, and pressure yielding well-established phase diagrams.[2] The order-to-disorder transition is driven by the degree of polymerization N and the Flory−Huggins segment interaction parameter χ. Surfaces and interfaces influence this phase separation process. Because of the different interactions between the interface and the blocks, one component segregates at the interface. As a consequence of this surface-induced ordering in thin films of block copolymers, a lamellar order is preferred for topological reasons, in particular if the composition is close to 50%. The lamellae are oriented parallel to the substrate surface which can be understood as the ordering field. The lamellar period L corresponds to the thickness of an ABBA or BAAB bilayer. As a function of decreasing film thickness, additionally, a reorientation of the lamellar domains from a parallel to a perpendicular arrangement was observed.[3] The internal order as well as the ordering of thin films of diblock copolymers was investigated with several experimental techniques[4−10] as well as theoretically.[11−14] Commonly, as-prepared thin films are obtained by spin-coating a diblock copolymer solution onto a substrate. During annealing above the glass transition temperature of the copolymer the internal order is installed.[8,15−18] The actual film thickness l determines the number of built-up lamellae as well as the creation of holes or islands due to a noninteger ratio of l/L. The minimization of the surface free energy density rules which block is present at the interfaces.

As-prepared samples right after the spin-coating were only rarely investigated as compared to ordered samples in the past. In the disordered state the copolymer microdomains may be randomly oriented with respect to the surface[15,16] or may show a lamellar order with different periodicity, as compared to the equilibrium bulk state,[17,18] while the surface of the thin films was reported to be essentially flat.[8,15,17] Previous investigations dealing with homopolymer films[19−21] as well as with polymer blend films[22] have shown that as-prepared films right after the spin-coating exhibit a very special type of surface roughness. The polymer−air interface replicated the substrate roughness over a large frequency range.[23] This roughness replication decays after annealing.[20] The presented investigation are focused on this long-range correlation in the case of thin diblock copolymer films. Because of the internal length scale introduced by the lamellar period L in the case of diblock copolymer films, a different behavior as compared to more simple polymers might be expected. Thus, we have chosen a model system that showed an internal ordering right after preparation, to emphasize on the influence of an internal structure. In the present investigation, we focus on typical key parameters like the molecular weight and the film thickness.

This article is structured as follows: The introduction is followed by an experimental section describing the sample preparation and the techniques used. The sections on results and discussion are followed by a summary and an outlook.

Experimental Section

Sample Preparation. For our experiments we used several different poly(styrene-*block*-*p*-methylstyrene) diblock copolymers, denoted P(S-*b*-pMS), with different molecular weights as listed in Table 1. To prepare thin films, a toluene solution was spin-coated (1950 rpm for 30 s) on top of native oxide covered Si(100) surfaces (MEMC Electronic Materials Inc., Spartanburg). Prior to the spin-coating, the substrates were cleaned in an acid bath. The cleaning bath consists of 100 mL of 80% H_2SO_4, 35 mL of H_2O_2, and 15 mL of deionized water.

† TU München.
‡ Institut f. Polymerforschung e.V.
§ Max-Planck-Institut für Polymerforschung.
* Corresponding author.

10.1021/ma002181v CCC: $20.00
Published on Web 09/07/2001

Table 1. Characteristic Data of the Diblock Copolymers Used in This Study[a]

sample	M_w (g/mol)	M_w(PS) (g/mol)	M_w(PpMS) (g/mol)	M_w/M_n
P42K	41 900	20 000	21 900	1.12
P62K	61 900	26 800	35 100	1.19
P84K	84 300	33 100	51 200	1.10
P123K	122 700	59 600	63 100	1.04
P230K	230 000	115 000	115 000	1.08

[a] Abbreviations used in the text: molecular weight M_w, molecular weight of the polystyrene block M_w(PS), molecular weight of the poly(*p*-methylstyrene) block M_w(PpMS), and polydispersity M_w/M_n.

After 15 min at 80 °C in the acid bath the substrates were taken out, rinsed in deionized water, and dried with compressed nitrogen. Immediately before coating the dry substrates were flushed with fresh toluene. The excess solvent was removed by one spinning cycle on the spin coater. From a variation of the polymer concentration of the solution used during the spin-coating the film thickness was altered.[24] We prepared film thicknesses between 25 and 1190 Å as determined by X-ray reflectivity. The annealing of the samples was performed in a vacuum furnace at $T = 161.8$ °C ex-situ and at $T = 195$ °C in-situ. In the case of ex-situ experiments after the chosen annealing time the samples were quenched down to room temperature, which is well below the glass transition temperature of both copolymers PS and PpMS, and examined. During in-situ experiments, the samples were examined after the desired annealing time above the microphase separation temperature $T_{MST} = 153 \pm 4$ °C of P230K.[4] To check the reproducibility of the reported results, several samples of each type were prepared and examined.

X-ray Reflectometry. Using X-ray reflectivity, the bare substrates were characterized and the initial film thicknesses of the polymer films were determined. These measurements were performed at the A2 polymer beamline of the DORIS III storage ring at HASYLAB/DESY in Hamburg at a wavelength $\lambda = 1.5$ Å. The sample is placed horizontally and mounted inside a vacuum chamber. From a fit to the reflectivity data, the density profile perpendicular to the sample surface is determined.[25−28] Thus, film thickness, surface roughness, and mean density of the diblock copolymer films are yielded.

Scanning Force Microscopy. The sample surface is investigated with scanning force microscopy (SFM) using a PARK Autoprobe CP atomic force microscope. The images are taken at air in the noncontact mode, which minimizes the tip-induced sample degradation. Micrographs were recorded at several different sample positions using scan ranges between 5 μm × 5 μm and 80 μm × 80 μm. We used gold coated silicon cantilevers with lengths of 180 μm, widths of 25 μm, and thicknesses of 2 μm. The force constant is approximately 2.1 N/m. The high aspect ratio conical tip has a typical radius of curvature of 100 Å. After the measurement the background due to the scanner tube movement is fully subtracted from the data to determine values of the rms surface roughness.

X-ray Off-Specular Scattering. The diffusely scattered intensity was recorded during measurements at the BW4 USAX beamline of the DORIS III storage ring at HASYLAB/DESY in Hamburg. The selected wavelength was $\lambda = 1.38$ Å. For further details concerning the beamline see ref 29. During common USAX experiments the instrument is used in transmission geometry. To detect off-specular scattering, we installed a two-circle goniometer with a *z*-translation table[30] and used a setup of high-quality entrance slits and a completely evacuated pathway. The beam divergence in and out of the plane of reflection was set by two entrance cross-slits. At a fixed incident angle of $\alpha_i = 1.02°$ and $\alpha_i = 1.23°$ the scattered intensity was recorded with a two-dimensional detector consisting of a 512 × 512 pixel array. A schematic picture of the setup used is shown in Figure 1. The two-dimensional intensity distribution consists of several vertical and horizontal slices. Cuts in vertical direction, at constant out-of-plane angles ψ, correspond to "detector scans" and "off-detector scans". Cuts in horizontal direction, at constant exit angles α_f, correspond to so-called "out-of-plane scans".[31−33] The (*xy*)-plane denotes the sample surface and $\vec{q} = (q_x, q_y, q_z)$ the scattering vector. A sample−detector distance of 2.87 m was chosen to obtain a relaxed resolution in out-of-plane direction ($\Delta q_y < 1 \times 10^{-3}$ Å^{-1}) because we restrict ourselves to vertical cuts. These cuts contain the desired information about any long ranged correlation perpendicular to the sample surface.

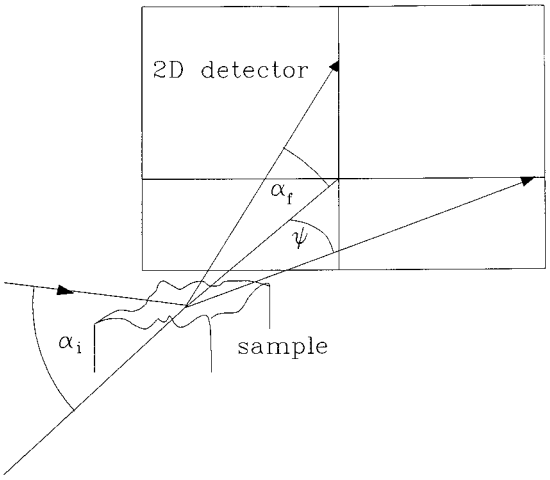

Figure 1. Schematic view of the experimental setup used for the off-specular X-ray scattering measurements. The incident angle is denoted α_i, the exit angle α_f, and the out-of-plane angle ψ. A two-dimensional detector is used to measure one complete set of data consisting of the detector scan and several off-detector scans at a given incident angle.

In a common "detector scan", the sample is held fixed at one angle of incidence α_i and the detector position is varied around the specular peak. According to $\Delta q_x \sim \pm(2\pi/\lambda)\alpha\Delta\alpha$ and $\Delta q_z \sim (2\pi/\lambda)\Delta\alpha$ the changes in the exit angle $\Delta\alpha$ will mainly result in a change of q_z and only very small changes in q_x. Thus, a "detector scan" basically probes vertical correlations.[23,34] In a q_xq_z map a detector scan is a parabolic path through the reciprocal space, which cuts the Yoneda[35] as well as the specular streak.[26] In a typical scan both are visible as peaks. The intensity depends on the roughness of the sample and the chosen incident angle α_i. In the case of correlated roughness[23] additional intensity streaks due to resonant diffuse scattering are present. These streaks are oriented parallel to the q_x-axis. Thus, in a detector scan they are observable as an additional modulation of the intensity.[19−23,34] From the spacing of these fringes the distance between the correlated interfaces can be estimated.

In an "off-detector scan" the sample is held fixed at one angle of incidence α_i, and the detector position is varied around the specular peak at a fixed out-of-plane angle ψ. Thus, in these scans is $q_y \neq 0$ Å^{-1}, which corresponds to paths through the reciprocal space shifted parallel to the parabolic path of a "detector scan" due to the additional q_y component. Basically "off-detector scans" exhibit similar features like in a "detector scan". The disappearance of the interference fringes in "off-detector scans" with increasing q_y value indicates that the top and bottom interface of the polymer film are no longer correlated. Thus, the smallest replicated in-plane length scale R_c can be estimated by successively measuring "off-detector scans" with increasing q_y. In our setup this is equivalent to several vertical cuts of the two-dimensional intensity with increasing q_y.

Results and Discussion

1. As-Prepared Samples. The X-ray reflectivity measurements of the samples right after preparation exhibit well-pronounced fringes and no sign of a Bragg peak within the measured *q* range. The Bragg peak will be difficult to resolve anyway because of the low electron

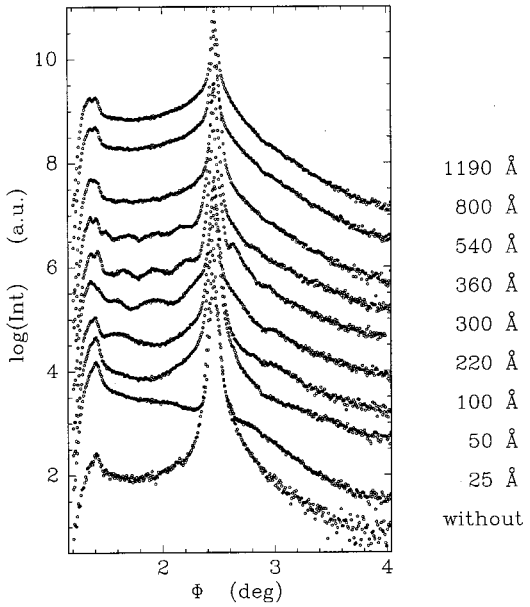

Figure 2. "Detector scans" measured at the angle of incidence $\alpha_i = 1.23°$ of the P230K films as prepared for different film thicknesses covering a range from 25 Å up to 1190 Å. The data of the bare substrate are shown as well (named "without"). For clarity, the curves are shifted by 1 order of magnitude against each other.

density difference between PS and PpMS. The film thickness l varied between 25 and 1190 Å. The determined film density equals the mean density of both components of the diblock copolymer PS and PpMS. The surface roughness is of the order of the substrate surface roughness. As the SFM experiments prove, the sample surface shows no marked features like terraces or islands. Thus, the copolymer−air interface is essentially flat and statistically rough. Now we focus on the roughness spectrum of the polymer surface in more detail:

To probe for possible roughness replication, we performed off-specular measurements at an angle of incident α_i above the critical angle of total reflection α_c of the polymer film (with $\alpha_i \gg \alpha_c$). Therefore, the typical characteristics of the scattered intensity (Yoneda peak, specular peak, modulations due to resonant diffuse scattering) can be easily separated. Figures 2 and 4 show cuts along the direction of a "detector scan". The detector angle is denoted with $\Phi = \alpha_i + \alpha_f$. In horizontal direction the intensity was integrated over $\Delta q_y = \pm 3.12 \times 10^{-3}$ Å^{-1}. In Figures 2 and 4 the Yoneda peak is observed at $\Phi_y = 1.41°$ and the specular peak at $\Phi_s = 2.45°$. Additional modulations of the intensity originate from resonant diffuse scattering.

a. Influence of Film Thickness. To figure out the influence of the film thickness, this parameter of the diblock copolymer film is varied using one fixed molecular weight. We prepared thin P(S-*b*-pMS) films with thicknesses between 25 and 1190 Å using a molecular weight of $M_W = 230\,000$ g/mol (P230K in Table 1) and a nearly symmetrical composition $f = N_{PS}/N = 0.47$. With small-angle neutron scattering experiments a radius of gyration of $R_g = 136$ Å[36,37] and a lamellar spacing of $L = 450$ Å[4,38] were determined for bulk samples of this molecular weight. Thus, in terms of the characteristic internal lengths of the investigated copolymer, the films are thin. With respect to the lamellar spacing they cover a range between $L/16$ and $11L/4$. The

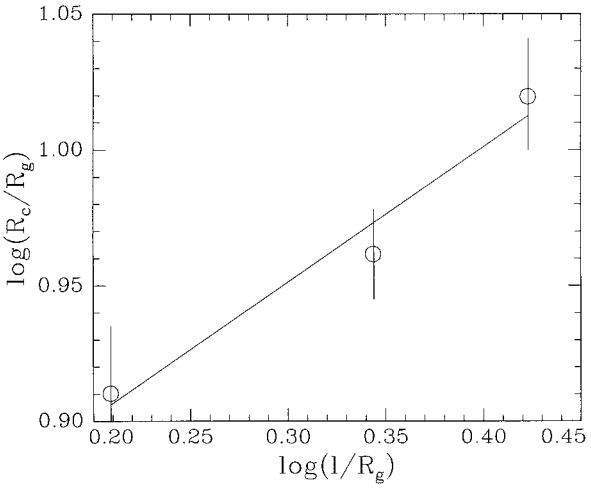

Figure 3. Double-logarithmic plot of the smallest replicated in-plane length scale R_c as a function of the total film thickness l right after preparation. The data are normalized by the radius of gyration R_g. The solid line is a fit to the data using a model, as explained in the text.

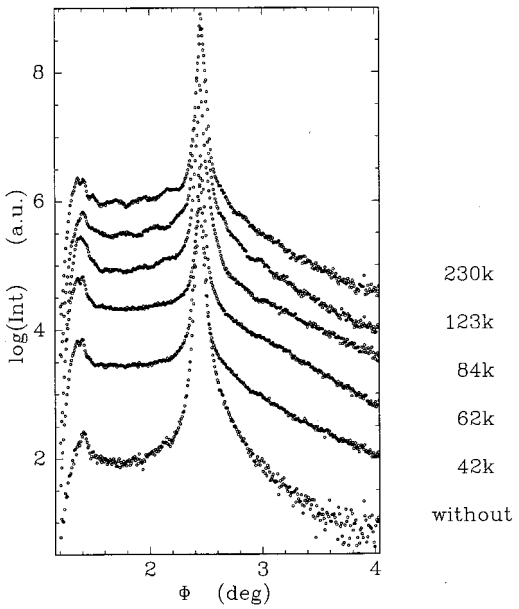

Figure 4. "Detector scans" measured at the angle of incidence $\alpha_i = 1.23°$ of films with a fixed film thickness $l = 350 \pm 12$ Å but different molecular weights between 42K and 230K. For clarity, the curves are shifted by 1 order of magnitude against each other.

investigated film thickness range is comparable to the range in which long-range correlation was observed in PS homopolymer films.[19,20] As known from these experiments at homopolymer samples, the strength of the long-range correlation decreases with increasing film thickness. Figure 2 shows that a similar behavior is observed in the P(S-*b*-pMS) films as well (the bare substrate is abbreviated "without"). But in general, the modulations observable in the copolymer films are weak as compared to the ones measured in the case of homopolymer films. Modulations due to resonant diffuse scattering are only present up to 360 Å. In contrast to for example polystyrene films at a film thickness of 540 Å, no sign of correlation was detectable in the P(S-*b*-pMS) films. It should be noted that this is not due to a limited resolution of our experimental setup, which would enable the detection of correlated roughness well

above 1500 Å.[30] The influence of the solvent used during the spin-coating process can be neglected since toluene is used as a common solvent for most of the investigations concerning roughness replication.[19−22] Thus, the long-range correlation as a function of film thickness in P(S-*b*-pMS) diblock copolymer films is different from that of PS homopolymer films. Expressed in terms of the radius of gyration it extends only over a much smaller thickness range as compared to homopolymers like polystyrene. We attribute this to the chemical structure of the diblock copolymer molecule which forces a phase separation into microdomains. Without annealing, right after preparation these micordomains are built up oriented parallel to the sample surface already.[17,38−40] Thus, P(S-*b*-pMS) behaves different as compared to diblock copolymer systems like P(S-*b*-MMA) which exhibit randomly oriented microdomains with respect to the surface.[15] The low surface energy of PpMS and the large difference in the surface energies of PS and PpMS forces a surface segregation of the PpMS block. Consequently, a surface-induced ordering is introduced which decays starting from the film surface after a few periods. The periodicity $\tilde{L}$ is only half of the bulk lamellar period L. In earlier investigations a value of $\tilde{L} = 240 \pm 10$ Å was determined[17,40] for thick P(S-*b*-pMS) films. The rest of the film consists of randomly oriented microdomains. The surface-induced ordering right after preparation was observed down to film thicknesses of $l = 7L/8 \cong 380$ Å.[39,40] Thus, we can attribute the absence of roughness replication to the presence of this lamellar ordering which resists the roughness transfer. The energy needed for bending of a lamellar structure is much larger as compared to the energy needed in the case of an absence of a parallel ordering. Via the randomly oriented microdomains near the substrate the lamellae near the surface are decoupled from the substrate surface. At a film thickness of $l = 2L/4 = 360$ Å the internal film structure is completely different. A creation of 1.5 lamella which would fit the film thickness is energetically extremely disadvantageouse because the PpMS block prefers both boundaries. The formation of islands is energetically avoided due to the big difference in the surface energies of both components PS and PpMS. Thus, as determined with ^{15}N nuclear reaction analysis, the PpMS block segregates to the surface and the PpMS contend decays monotonically without any internal ordering.[40] The microdomains are randomly oriented. Consequently, at this film thickness we observed roughness replication. The diblock copolymer film behaves comparably to a homopolymer film. In the case of film thicknesses smaller than one as prepared lamella $\tilde{L} =$ 240 Å no ordering parallel to the substrate is possible as well.[40] A further compression of the lamellar spacing seems to be impossible due to the geometrical dimension of blocks and only surface segregation of PpMS was reported. Again, we observe correlated roughness in this film thickness regime resulting from the absence of oriented lamellae. In general, the roughness replication in P(S-*b*-pMS) diblock copolymer films is weaker as compared to PS homopolymer films due to the presence of randomly oriented microdomains inside the film. Nevertheless, a part of the roughness spectrum is transferred.

For equilibrium conditions roughness correlation of thin films is described within the framework of a linear response theory by Andelmann et al.[41] The roughness spectrum of the substrate is partially transferred through the thin film. Like a band-pass filter the long wavelength fluctuations of the solid surface are followed by the film surface, and short wavelength fluctuations are damped out by surface tension. In general, with increasing film thickness the film surface becomes smoother and undulations of the solid surface are followed more closely as the film thickness decreases. However, thin films prepared by spin-coating are not in their equilibrium state, and thus the theory of Andelmann et al. is not applicable for our investigation. In the case of glassy homopolymer films the surface morphology right after preparation by spin-coating is described as a frozen liquid.[20] Thus, the smallest replicatable in-plane length scale R_c depends on the film thickness l following $R_c \sim l^{0.5}$ [20,42] due to the bending rigidity of the surface.[43,44] The polymer surface behaves conformally to the roughness of the substrate for in-plane lengths $R > R_c$. In Figure 3 the smallest replicated length scale R_c is plotted as a function of the film thickness l. To relate the results to typical polymer dimensions, both lengths are normalized by the radius of gyration R_g of the unperturbed chains. Only data from samples that enable a doubtless determination of R_c are taken into account. Consequently, we restrict ourselves to three different film thicknesses and skip the three others in the small film thickness regime, which exhibit modulations difficult to detect in the off-detector scans. Although the experiments were performed with synchrotron radiation the scattering in this out-of plane direction is extremely weak. Nevertheless, within the limited range the measured data are compatible with $R_c \sim l^{0.5}$ (solid line in Figure 3). This suggests that also in the case of diblock copolymers right after preparation the surface morphology is describable as a frozen liquid. However, a distortion with an in-plane wavenumber $q = 2\pi/R_c$ decays stronger in the z-direction as compared to homopolymer films. Thus, the chemical linkage of incompatible polymers does only effect the strength of roughness replication but not its scaling.

b. Influence of Molecular Weight. The second parameter describing a copolymer addressed in this investigation is the molecular weight. At a fixed film thickness of $l = 350 \pm 12$ Å films out of different diblock copolymers, as listed in Table 1, were examined. The error bar denotes the variation of the film thickness within the several sample series examined. Roughly all diblock copolymers used are symmetric with a styrene fraction of the copolymer of $f = N_{PS}/N = 0.47 \pm 0.04$. In Figure 4 the corresponding detector scans are shown. For comparison, the data of the bare substrate are shown again (marked "without"). In the data of the low molecular weight films P42K and P62K no sign of roughness correlation is detectable. With increasing molecular weight from 84K to 230K the amplitude of the modulation resulting from resonant diffuse scattering increases. Nevertheless, as compared to homopolymer films, the roughness replication is reduced again.[19] In the case of diblock copolymers the change in the molecular weight M_w changes several important parameters: Due to the small incompatibility between the molecules PS and PpMS, which monomers differ both only by one methyl group, the installation of order is effected. The polymer−polymer interaction parameter of PS and PpMS is $\chi = A + B/T$ with $A = -0.011 \pm 0.002$ and $B = 6.8 \pm 1$ K.[45] Thus, only the sample P230K belongs to the strong segregation regime, the sample

P123K belongs to the weak segregation regime, and the samples P84K, P62K, and P42K are disordered. In the strong segregation limit the lamellar spacing follows $L \sim N^{2/3}$ where N denotes the degree of polymerization.[11,46] Thus, a change in the molecular weight leads to the absence or presence of lamellae and the lamellar spacing L is modified as well. At a constant film thickness l the ratio l/L increases with decreasing molecular weight. However, all these morphologies are related to the equilibrium case. Consequently, it is not surprising that neither the change in the segregation limit nor the nonconstant ratio of l/L can explain the observed presence of roughness replication within the range between 84K and 230K. During the preparation via spin-coating the mobility of the chains is responsible for the buildup of the energetically unfavorable morphology related with the roughness replication.[20] Entanglements restrict the mobility of the molecules in the bulk and in concentrated solutions, as they occur due the evaporation of the solvent during the spin-coating. Qualitatively, an entanglement can be envisioned as a crossing of polymer chains which remains intact and hence mechanically active, when subjected to a strain. Consequently, as-prepared polystyrene films below the entanglement molecular weight $M_e = 18\,100$ g/mol of PS[47] exhibit no roughness replication.[19] In all of the investigated diblock copolymers the molecular weight of one block is above this value. On the other hand, in diblock copolymers due to the internal chemical structure of the molecule, the value of the entanglement molecular weight is larger as compared to the corresponding homopolymer. The chemical linkage of both blocks yields only one free chain end and a limited flexibility because the individual block try to avoid a crossing. Thus, at a fixed chain length the probability for the crossing of the polymer chains in the melt state is reduced, as compared to the homopolymer. Below the entanglement molecular weight the polymer melt behaves more like a liquid than a polymer. It should be noted that viscosity also depends strongly on molecular weight.[44] Consequently, one might address the absence of roughness replication in the low molecular weight regime of diblock copolymers following the same mechanisms as in homopolymer films.

2. Annealed Samples. Within all annealing experiments we restrict ourselves to measurements using the diblock copolymer films with the highest molecular weight P230K. As taken from the molecular weight dependence these samples exhibit the strongest intensity modulations in the resonant diffuse scattering. A reasonable strong signal is required for the determination of its decrease due to the decay of the long-range correlation.

Changes of the density profile perpendicular to the sample surface are followed by in-situ X-ray reflectivity measurements during the annealing at a temperature of $T = 195$ °C. This annealing temperature is well above the glass transition temperature of both components of the diblock copolymers and above the microphase separation temperature $T_{MST} = 153 \pm 4$ °C.[4,36,37] Thus, the copolymer is annealed in its disordered state. The sample is subsequently shifted perpendicular to the X-ray beam to avoid any radiation damage. As we focus during this investigation on the early stages of film creation in diblock copolymer films, the annealing is restricted to 15.4 h. The relative change in the film thickness l_t/l as a function of the annealing time is shown in Figure 5 for the example of a film with an originally prepared film thickness $l = 314$ Å. After the onset of annealing, which marks the zero of the time axis, first the film thickness l_t reduces slightly as compared to l. Next, during in-situ annealing it increases without reaching the originally prepared value l. After roughly 4 h annealing the film thickness stays unchanged. It has to be noted that all changes are extremely small. As reported in ref 4, 24 h annealing at $T = 160$ °C is sufficient for the buildup of the lamellar ordering. Applying the frequently used Williams−Landell−Ferry equation,[49,50] this corresponds to 0.97 h at our chosen annealing temperature $T = 195$ °C. Nevertheless, we might attribute the change in the observed film thickness to the internal ordering of the film. Of course, no sign of a Bragg peak is detectable from the measured films due to the extremely small film thickness and the small electron contrast. One would need at least a lamellar stacking consisting of several lamellae to obtain an enhanced scattering at the position of the Bragg peak. After the annealing the samples are quenched down to room temperature and examined with SFM. However, in all accessed scan ranges we did not detect any sign of morphologies like holes or islands on top of the film. The copolymer films still remain homogeneous. This is in good agreement with the very small changes on the order of a few angstroms in the surface roughness determined from the X-ray data. Thus, during the annealing the internal ordering is installed without characteristic surface features. In accordance with previous experiments[4] and with the relation of the surface tensions $\gamma(\text{PpMS})/\gamma(\text{PS}) = 0.86$,[48,51] the fit to the data suggests that the surface is covered with PpMS.

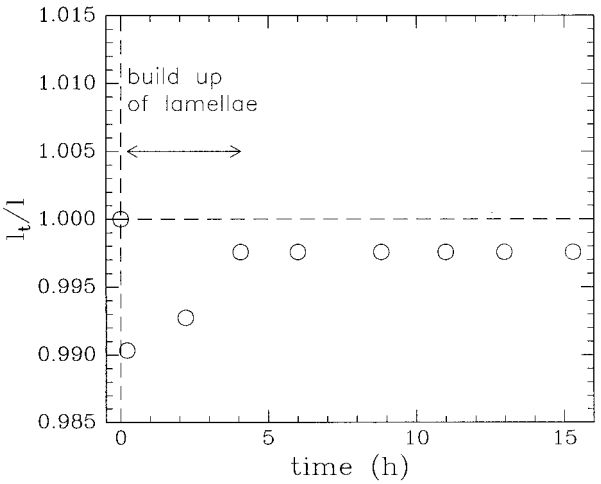

Figure 5. Relative change in the film thickness l_t/l during in-situ annealing at $T = 195$ °C. The dashed line represents the originally prepared film thickness as detected right after preparation. The shown data belong to an example film thickness of $l = 314$ Å.

a. Decay of Long-Range Correlation. Focusing the decay of roughness replication, we performed off-specular measurements again. The incident angle is chosen above the critical angle to make a separation between the typical characteristics of the scattered intensity (Yoneda peak, specular peak, modulations due to resonant diffuse scattering) easier. We reduce the angle of incidence as compared to measurements presented above to increase the intensity and improve the statistics. Thus, in Figures 6 and 7 the Yoneda peak is observed at $\Phi_y = 1.19°$ and the specular peak at $\Phi_s =$

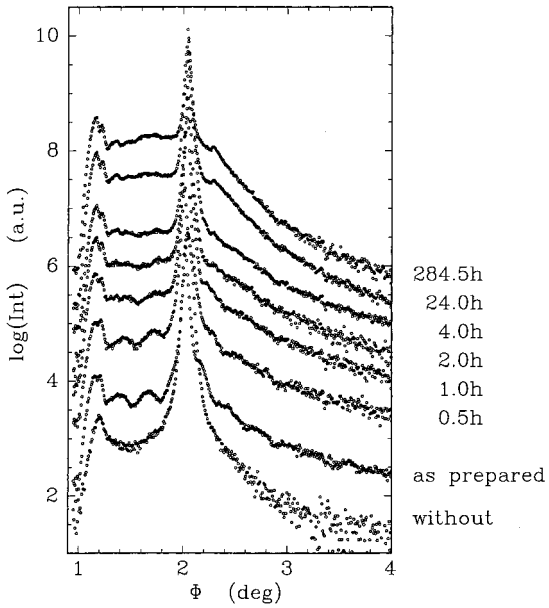

Figure 6. "Detector scans" measured at the angle of incidence $\alpha_i = 1.01°$ of films annealed ex-situ at $T = 161.8$ °C for different times. The film thickness is $l = 300 \pm 5$ Å and the molecular weight 230K. For clarity, the curves are shifted by 1 order of magnitude against each other.

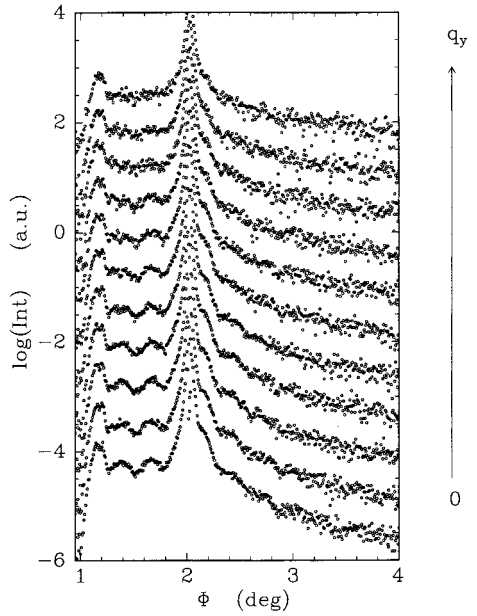

Figure 7. "Off-detector scans" showing the evolution of the modulation resulting from resonant diffuse scattering as a function of increasing q_y (from the bottom to the top). For clarity, the curves are shifted by 1 order of magnitude against each other.

2.04°. In horizontal direction the intensity was integrated over $\Delta q_y = \pm 3.12 \times 10^{-3}$ Å^{-1} as well.

We enhanced the time resolution of the examination by choosing a reduced annealing temperature of $T = 161.8$ °C as compared to the in-situ experiments. A further reduction of the annealing temperature was not possible because the annealing should be performed well above the microphase separation temperature T_{MST} of P230K. Nevertheless, the long experimental time required for a set of detector and off-detector scans which is on the order of 3 h forces these ex-situ experiments. The samples were quenched to room temperature after annealing for 0.5, 1, 2, 4, 24, and 284.5 h. In Figure 6 the "detector scans" of the annealed samples with a film thickness of $l = 300$ Å are shown in comparison to the one measured right after preparation (marked "as prepared") and to the bare substrate (marked "without"). Modulations resulting from resonant diffuse scattering are observable over a time interval during the annealing. As usually observed in the case of homopolymer films as well[19−21] right after annealing above the glass transition temperature, the modulation due to resonant diffuse scattering becomes weaker. As long as the system stays glassy, no relaxation is possible. In the melt the molecules are able to move. The damping of the modulations is visible at larger detector angles Φ first; the amplitude of the diffuse modulation reduces as a function of annealing time. This amplitude can be taken as an indication for the strength of the interface correlation, since during the annealing experiment the differences in the mean electron density remain unchanged, despite small changes of the density due to thermal expansion. After 4 h it is vanished without any reinstallation because roughness replication forces the polymer molecules into a energetically unfavored state. After 24 h the shape of the "detector scan" again changed which is due to the completed built up of the internal lamellar structure. This is in good agreement with previous observations using ^{15}N nuclear reaction analysis which showed that 24 h of annealing at $T = 160$ °C is sufficient for the buildup of the lamellar ordering with the bulk lamellar spacing.[4] After 284.5 h of annealing which would correspond to 14.3 h at $T = 195$ °C no further changes are detectable. Thus, in terms of perpendicular correlations the diblock copolymer film remains unchanged over this annealing time. The slight relaxation in the film thickness, as observed with reflectivity measurements, up to 4 h annealing at $T = 195$ °C has no correspondence in the "detector scans". This results in the different properties of the sample probed with both techniques. Both techniques as well as additional SFM measurements show that the copolymer films are still homogeneous after the long annealing. Nevertheless, this homogeneous film does not correspond to the equilibrium structure. After sufficient long annealing the film starts to dewet the substrate.[52] Consequently, we cannot extract the smallest replicated in-plane length scale R_c as a function of the total film thickness after preparation l for the equilibrium surface morphology similar to the data presented in Figure 3. The kinetics in the system are quite slow due to the large molecular weight. The dewetting goes beyond the desired investigation of the early stages of film creation and is therefore not examined further.

b. Morphology Changes. Accessing the "off-detector scans" the time-dependent increase of the short-wavelength cutoff R_c describing the changes in the surface morphology was measured. Figure 7 shows these "off-detector scans" for a film thickness of $l = 300$ Å. From the bottom to the top q_y increases in steps of $\Delta q_y = 5.6 \times 10^{-4}$ Å^{-1}. The curves are shifted against each other for clarity. The amplitude of the fringes resulting from resonant diffuse scattering decreases with increasing q_y. This indicates the loss of correlation at smaller in-plane length scales while at long in-plane length scales the substrate and the polymer−vacuum interface are still correlated. The typical time constant observed in the experiment suggests a diffusion driven mechanism. The related length scales of the surface rms roughness and the in-plane correlation length differ at

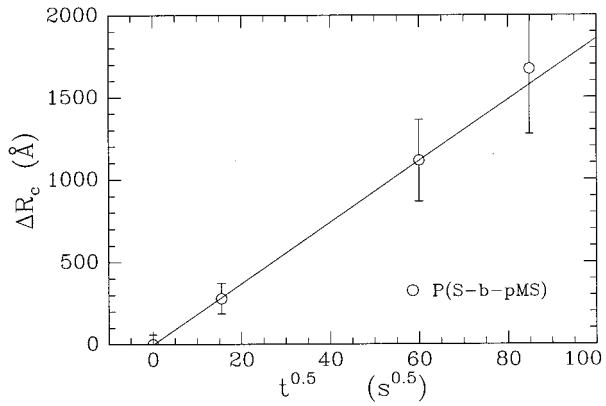

Figure 8. In-situ measurement of the relaxation of the smallest replicatable in-plane length scale ΔR_c as a function of the annealing time t. The annealing at $T = 161.8$ °C was started at $t = 0$. The film thickness of the sample examined is $l = 300 \pm 5$ Å. The solid line is based on a model calculation, as explained in the text.

least by 2 orders of magnitude. Thus, the three-dimensional movement can be understood as a basically two-dimensional one. The measured diffusion in direction of decaying concentration is described by a surface diffusion $\Delta R_c \sim \sqrt{4D_s t}$ with a surface diffusion coefficient D_s. The changes in the smallest replicatable length scale R_c as a function of the annealing time $t^{0.5}$ are shown in Figure 8. Within this typical diffusion plot our data are describable by a linear dependence (solid line in Figure 8). From the slope a value of $D_s = 8.7 \times 10^{-15}$ cm^2/s is obtained. Compared to previous experiments on brominated polystyrene films on top of silicon surface ($D_s = 9.3 \times 10^{-16}$cm^2/s, $M_w = 145$K[20]), this value is 10 times larger. Thus, the diffusion in the investigated diblock copolymer film is quicker although the film thickness is basically the same. This might be attributed to the reduced interaction of the polymer chains with the substrate as well as to the additional differences in the internal structure of the molecules. In addition, the molecular weight of the examined diblock copolymer is larger which slows down the kinetics. In thick P(S-*b*-pMS) films of the equal molecular weight and block ratio local diffusion coefficients between $D = 2 \times 10^{-16}$cm^2/s and $D_s = 5 \times 10^{-15}$cm^2/s were reported,[40] which is in good agreement with our observations. Unfortunately, no literature values about bulk diffusion constants of the diblock copolymer P(S-*b*-pMS) are known to the authors. Compared to common bulk diffusion constants of the related homopolymers PS and PpMS which are on the order of $D \cong 4 \times 10^{-14}$ cm^2/s,[49] the movement is slowed down. Similar observations were reported from homopolymer samples.[18,53,54] In the bulk the copolymers are surrounded by polymer molecules as well. If the copolymers are confined into a thin film geometry, the interactions with the boundaries influence the morphology and the kinetics.[55,56]

Summary and Outlook

With the presented experiments we addressed the early stages of film creation in diblock copolymer films. Roughness replication was detected within a limited film thickness, and molecular weight range in the case of as-prepared films. Thus, the spin-coating techniques enables the preparation of conformally rough copolymer films. Only a part of the roughness spectrum of the substrate is transferred through the film. At a short wavelength the replicated turns into a statistically independent roughness spectrum. For large wavelengths within the limited experimental resolution the substrate−polymer and the polymer−vacuum interface are correlated. Because of the chemical structure of the molecules and their tendency to build up oriented morphologies, the range of correlated roughness is reduced as compared to homopolymer films. The creation of lamellae aligned parallel to the substrate surface is the underlaying mechanism to persist the transfer of roughness contributions. Like in the case of homopolymer samples the surface morphology induced during the spin-coating process is dominated by bending elasticity of the freezing polymer solution in the case of extremely small film thicknesses. For larger film thicknesses an internal lamellar ordering is installed right after preparation. Equilibrium conditions are only reached within very long time scales during annealing. On short time scales of the annealing process the long-range correlation installed by the roughness replication is destroyed. Next, the internal lamellar orientation comparable to the bulk morphology is created. The order stays stable during a long annealing time, but the interaction with the underlying substrate forces a dewetting as a final morphology dominating step. This is of course no longer related to the early stages. The movement of the copolymer molecules during the decay of the long-range correlation is diffusion driven. The determined diffusion constant is larger as compared to homopolymer films, and diffusion is still slowed down as compared to that of bulk samples.

Acknowledgment. We thank S. Cunis and G. von Krosigk for the technical assistance at the BW4 beamline and A. Meyer and R. Döhrmann for their help at the A2 beamline at the HASYLAB. Additionally, we owe many thanks to R. Gehrke for his general support of the experiments at HASYLAB. This work was supported by the BMBF (Förderkennzeichen 03DUOTU1/4). B.M. was supported by DFG Grant IIC10-322 1009, and C.L-.H. was supported by Graduiertenkolleg Physik und Chemie Supramolekularer Systeme at Mainz University.

References and Notes

(1) Hamley, I. W. *The Physics of Block Copolymers*; Oxford University Press: New York, 1998.
(2) Alexandridis, P.; Spontak, R. J. *Curr. Opin. Colloid Interface Sci.* **1999**, *4*, 130.
(3) Morkved, T. L.; Jaeger, H. M. *Europhys. Lett.* **1997**, *40*, 643.
(4) Giessler, K.-H.; Rauch, F.; Stamm, M. *Europhys. Lett.* **1994**, *27*, 605.
(5) Stocker, W.; Beckmann, J.; Stadler, R.; Rabe, J. P. *Macromolecules* **1996**, *29*, 7502.
(6) Mansky, P.; Russell, T. P.; Hawker, C. J.; Pitsikalis, M.; Mays, J. *Macromolecules* **1997**, *30*, 6810.
(7) Torikai, N.; Noda, I.; Karim, A.; Satija, S. K.; Han, C. C.; Matsushita, Y.; Kawakatsu, T. *Macromolecules* **1997**, *30*, 2907.
(8) Vignaud, G.; Gibaud, A.; Grübel, G.; Joly, S.; Ausserre, D.; Legrand, J. F.; Gallot, Y. *Physica B* **1998**, *248*, 250.
(9) Mansky, P.; Tsui, O. K. C.; Russell, T. P.; Gallot, Y. *Macromolecules* **1999**, *32*, 4832.
(10) Heier, J.; Sivaniah, E.; Kramer, E. J. *Macromolecules* **1999**, *32*, 9007.
(11) Fredrickson, G. H. *Macomolecules* **1987**, *20*, 2535.
(12) Turner, M. S. *Phys. Rev. Lett.* **1992**, *69*, 1788.
(13) Fischer, M. E.; Nakanishi, H. *J. Chem. Phys.* **1981**, *75*, 5857.
(14) Tang, W. H. *Macromolecules* **2000**, *33*, 1370.
(15) Coulon, G.; Russell, T. P.; Deline, V. R.; Green, P. F. *Macromolecules* **1989**, *22*, 2581.

(16) Russell, T. P.; Coulon, G.; Deline, V. R.; Miller, D. C. *Macromolecules* **1989**, *22*, 4600.
(17) Giessler, K.-H.; Endisch, D.; Rauch, F.; Stamm, M. *Fresenius J. Anal. Chem.* **1993**, *346*, 151.
(18) Bates, F. S.; Fredrickson, G. H. *Annu. Rev. Phys. Chem.* **1990**, *41*, 515.
(19) Müller-Buschbaum, P.; Stamm, M. *Macromolecules* **1998**, *31*, 3686.
(20) Müller-Buschbaum, P.; Gutmann, J. S.; Lorenz, C.; Schmitt, T.; Stamm, M. *Macromolecules* **1998**, *31*, 9265.
(21) Müller-Buschbaum, P.; Gutmann, J. S.; Kraus, J.; Walter, H.; Stamm, M. *Macromolecules* **2000**, *33*, 569.
(22) Gutmann, J. S.; Müller-Buschbaum, P.; Schubert, D. W.; Stribeck, N.; Smilgies, D.; Stamm, M. *Physica B* **2000**, *283*, 40.
(23) Holý, V.; Baumbach, T. *Phys. Rev. B* **1994**, *49*, 10668.
(24) Schubert, D. W. *Polym. Bull.* **1997**, *38*, 177.
(25) Parrat, L. G. *Phys. Rev.* **1954**, *55*, 359.
(26) Born, M.; Wolf, E. In *Principles of Optics*, 2nd ed.; Pergamon Press: Oxford, 1964.
(27) James, R. W. In *The Optical Principles of the Diffraction of X-rays*; OxBow Press: Woodbridge, CT, 1962.
(28) Stamm, M.; Schubert, D. W. *Annu. Rev. Mater. Sci.* **1995**, *25*, 325.
(29) Gehrke, R. *Rev. Sci. Instrum.* **1992**, *63*, 455.
(30) Müller-Buschbaum, P.; Casagrande, M.; Gutmann, J. S.; Kuhlmann, T.; Stamm, M.; Cunis, S.; von Krosigk, G.; Lode, U.; Gehrke, R. *Europhys. Lett.* **1998**, *42*, 517.
(31) Salditt, T.; Rhan, H.; Metzger, T. H.; Peisl, J.; Schuster, R.; Kotthaus, J. P. *Z. Phys. B* **1995**, *96*, 227.
(32) Salditt, T.; Metzger, T. H.; Peisl, J.; Goerigk, G. *J. Phys. D*: *Appl. Phys.* **1995**, *28*, A236.
(33) Salditt, T.; Metzger, T. H.; Brandt, Ch.; Klemradt, U.; Peisl, J. *Phys. Rev. B* **1995**, *51*, 5617.
(34) Daillant, J.; Bélorgey, O. *J. Chem. Phys.* **1992**, *97*, 5824.
(35) Yoneda, Y. *Phys. Rev.* **1963**, *131*, 2010.
(36) Jung, W. G.; Fischer, E. W. *Macromol. Chem. Macromol. Symp.* **1988**, *16*, 281.
(37) Bartels, V. T.; Abetz, V.; Mortensen, K.; Stamm, M. *Europhys. Lett.* **1994**, *27*, 371.
(38) Götzelmann, A.; Ph.D. Thesis, Mainz University, 1993.
(39) Stamm, M.; Götzelmann, A.; Giessler, K.-H.; Rauch, F. *Prog. Colloid Polym. Sci.* **1993**, *91*, 101.
(40) Giessler, K.-H. Ph.D. Thesis, Frankfurt University, 1996.
(41) Andelman, D.; Joanny, J. F.; Robbins, M. O. *Europhys. Lett.* **1988**, *7*, 731.
(42) Poniewierski, A.; Holyst, R. *Phys. Rev. B* **1993**, *47*, 9840.
(43) Keller, J. B.; Merchant, G. J. *J. Stat. Phys.* **1991**, *63*, 1039.
(44) Daillant, J.; Bosio, L.; Harzallah, B.; Benattar, J. J. *J. Phys. II* **1991**, *1*, 149.
(45) Schnell, R.; Stamm, M. *Physica B* **1997**, *234*−*236*, 247.
(46) Anastasiadis, S. H.; Russell, T. P.; Satija, S. K.; Majkrzak, C. F. *Phys. Rev. Lett.* **1989**, *62*, 1852.
(47) Ferry, J. D. In *Viscoelastic Properties of Polymers*; John Wiley & Sons: New York, 1980.
(48) Brandrup, J.; Immergut, E. H. In *Polymer Handbook*, 3rd ed.; John Wiley & Sons: New York, 1989.
(49) Green, P. F.; Kramer, E. J. *J. Mater. Res.* **1986**, *1*, 202.
(50) Tassin, J. F.; Monnerie, L.; Fetters, L. J. *Macromolecules* **1988**, *21*, 2404.
(51) Schnell, R. Ph.D. Thesis, University of Mainz, 1997.
(52) Müller-Buschbaum, P.; Gutmann, J. S.; Lorenz-Haas, C.; Wunnicke, O.; Stamm, M.; Petry, W., to be published.
(53) Zheng, X.; Sauer, B. B.; van Alsten, J. G.; Schwarz, S. A.; Rafailovich, M. H.; Sokolov, J.; Rubinstein, M. *Phys. Rev. Lett.* **1995**, *74*, 407.
(54) Zheng, X.; Rafailovich, M. H.; Sokolov, J.; Strzhemechny, Y.; Schwarz, S. A.; Sauer, B. B.; Rubinstein, M. *Phys. Rev. Lett.* **1997**, *79*, 241.
(55) Geisinger, T.; Müller, M.; Binder, K. *J. Chem. Phys.* **1999**, *111*, 5241.
(56) Geisinger, T.; Müller, M.; Binder, K. *J. Chem. Phys.* **1999**, *111*, 5251.

MA002181V